Desalination and Water Treatment
www.deswater.com
doi: 10.1080/19443994.2015.1025438

57 (2016) 8942–8951
April

Taylor & Francis
Taylor & Francis Group

EDTA- and amine-functionalized graphene oxide as sorbents for Ni(II) removal

Caiyun Zhao[a], Lingjuan Ma[a], Jinmao You[a], Fengli Qu[a,b,*], Rodney D. Priestley[b]

[a]*College of Chemistry and Chemical Engineering, Qufu Normal University, Qufu, Shandong 273165, P.R. China, Tel. +86 537 4456305; emails: caiyun.zhao@126.com (C. Zhao), qflhn@126.com (L. Ma), jmyou6304@126.com (J. You), fengliquhn@hotmail.com (F. Qu)*

[b]*Department of Chemical and Biological Engineering, Princeton University, Princeton, NJ 08544, USA, Tel. +1 609 258 5721; email: rpriestl@princeton.edu (R.D. Priestley)*

Received 8 October 2014; Accepted 20 February 2015

ABSTRACT

The adsorption behavior of Ni(II) onto graphene oxide (GO) derivatives N-(trimethoxysilylpropyl) ethylenediaminetriacetic acid-modified GO (EDTA-GO) and 3-Tri-methoxysilylpropyl-diethylenetriamine (amine–silane)-modified GO (amine-GO) were investigated. The EDTA and amine groups significantly enhanced the Ni(II) adsorption capacity of GO. The experimental results illustrated that GO-based sorbents could selectively remove Ni(II) from contaminated water with a maximum adsorption capacity of 103 mg/g within 30–45 min. The influence of pH on the adsorption/desorption properties as well as reusability of the modified GO derivatives was also investigated. These results demonstrate the application of modified GO as an effective adsorbent for water protection.

Keywords: Graphene oxide; Adsorption; Nickel

1. Introduction

Water is essential and plays a prominent role in human life. Due to the demands of industrialization and urbanization, water quality has been adversely affected by the contamination of heavy metals including nickel (Ni), cadmium (Cd), chromium (Cr), mercury (Hg), lead (Pb), and arsenic (As) [1]. Removing these metal contaminants from process wastewater prior to release is necessary to protect the environment because this kind of pollution is highly persistent, toxic, and tends to bioaccumulate in food chains [2–4]. This is problematic for human health, for instance, trace nickel in water can bind to nucleic acids and produce significant genetic effects [5,6].

In recent years, tremendous effort has been undertaken to develop new techniques and sorbents for water treatment [7]. An ideal sorbent should have the ability to remove toxic contaminants rapidly and efficiently from water to a safe level. Recent studies have demonstrated that carbon-based nanomaterials, such as carbon nanotubes (CNTs), are superior sorbents for the removal of heavy metal pollutants from water with high capacity and selectivity [8–12]. Among various carbon-based adsorbents, graphene oxide (GO), a free-standing two-dimensional atomic crystal, is potentially an ideal material for wastewater treatment. The unique physical and chemical properties of GO make it promising for potential applications in many fields [13–19].

*Corresponding author.

Unlike CNTs, which require a special oxidation process to introduce hydrophilic groups for heavy metal removal, the production process of GO from graphite inherently introduces the functional groups of –COOH, –C=O, and –OH on to the surface, which are favorable chemical functionalities for an ideal sorbent [20–32]. Recently, it was demonstrated that the silylation of GO is another efficient method to introduce efficient groups onto the surface of GO for the application of heavy metal removal from water [33]. For example, GO modified with N-(trimethoxysilylpropyl) ethylenediamine triacetic acid (EDTA–silane) via a silylation reaction can produce GO derivative of EDTA-GO [34,35]. The adsorption behavior of EDTA-GO for Pb(II) removal was examined and EDTA-GO was found to be an ideal adsorbent for Pb(II) removal with a higher adsorption capacity because of the chelating ability of ethylenediaminetriacetic acid [36]. Here, the adsorption behavior of Ni(II) on EDTA-GO and, another GO derivative, 3-Tri-methoxysilyl-propyl-diethylenetriamine (amine–silane)-modified GO (amine-GO) was investigated. We show that the modified GO can serve as an effective adsorbent for the removal of Ni from water.

2. Experimental section

2.1. Materials and equipment

Graphite, activated carbon powders (AC), hydrochloric acid, standard Ni(II) solution (1.0×10^3 mg/mL in double-distilled water), standard Cu(II) solution (1.0×10^3 mg/mL in double-distilled water), ion-exchange resin (DOWEX 50wx4-400), and other chemicals used in the experiments were purchased from Sigma-Aldrich, and used without further purification. Ni(II) solutions at various pH conditions were prepared by directly diluting the 1.0×10^3 mg/mL Ni(II) solution with a buffer solution prepared from KH_2PO_4–Na_2HPO_4 and NH_4Cl.

GO was obtained through natural graphite oxidation based on the Hummer's method [37]. As shown in Fig. 1, modified GO was prepare by treating GO with EDTA–silane or amine–silane in an ethanol solution [36]. In general, the silanization process consisted of dispersing 20.0 mg of GO into a three-neck flask with 150.0 mL ethanol using ultrasonication followed by the addition of 2 mL of 1.0 wt.% ethanol solution of EDTA–silane or amine–silane that was subsquently stirred for 12 h at 75°C [33]. The products were filtrated and dried in a vacuum at room temperature. In this experiment, the mass percent of Si in EDTA-GO is determined to be 5.8 ± 0.5 wt.% and the mass percent of Si in amine-GO is determined to be 4.2 ± 0.7 wt.%.

The concentration of metal ions in solution was analyzed using a Thermal Fisher Evolution 300 UV–Vis spectrum instrument and a Thermo Scientific ICAP 6000 Series inductively coupled plasma (ICP) system. The SEM and EDXS data were taken on a JEOL 2010F microscope (JEOL Ltd., Japan) with an energy dispersion X-ray (EDXS) analyzer. The sample separation was achieved using a Thermo Scientific Sorvall centrifuge. Fourier transform infrared (FTIR) spectrometry (Perkin–Elmer Spectrum One, USA) was used to characterize the structure changes of EDTA-GO, amine-GO, and GO, which were separately pressed into pellets with potassium bromide and then scanned from 500 to 4,000 cm^{-1} at a resolution of 4 cm^{-1}.

2.2. Adsorption experiments

A typical adsorption experiment was carried out by adding 20 mg of EDTA-GO or amine-GO to a 20 mL aqueous solution containing Ni(II) in a plastic vial at room temperature (25 ± 2°C) (named as dosage 20 mL/20 mg). The initial Ni(II) concentrations varied from 1 to 200 ppm and the pH value of all the solutions were maintained at pH 6.5 with a buffer solution. After adding the EDTA-GO or amine-GO, the vial with solution was sealed and left for 12 h to achieve the adsorption equilibrium state. Then the mixture was filtered through a 0.2 μm pore size membrane. The final Ni(II) concentration was analyzed using a UV spectrometry or ICP, and was identified as the equilibrium concentration (C_e). The amount of Ni(II) adsorbed was taken as the difference between the initial and equilibrium concentrations of Ni(II) in the solutions and the adsorption capacity (q_e, mg/g) of the Ni(II) adsorbed onto the EDTA-GO or amine-GO was obtained from Eq. (1):

$$q_e = \frac{(C_i - C_e) \times V}{w} \tag{1}$$

where C_i and C_e are the initial and equilibrium concentrations of Ni(II) (mg/L), V is the volume of Ni(II) solution (L), and w is the mass of EDTA-GO or amine-GO adsorbent (g).

The investigation of the adsorption kinetics was performed in a 50 mL solution containing 100 mg/L of Ni(II) with 20 mg of GO derivatives. The time used was recorded immediately when sorbents were mixed with Ni(II) solution and then were filtered immediately through a 0.2 μm membrane after a giving time. The amount of metal ions remained in the solution was determined and the adsorbed Ni(II) on GO derivatives

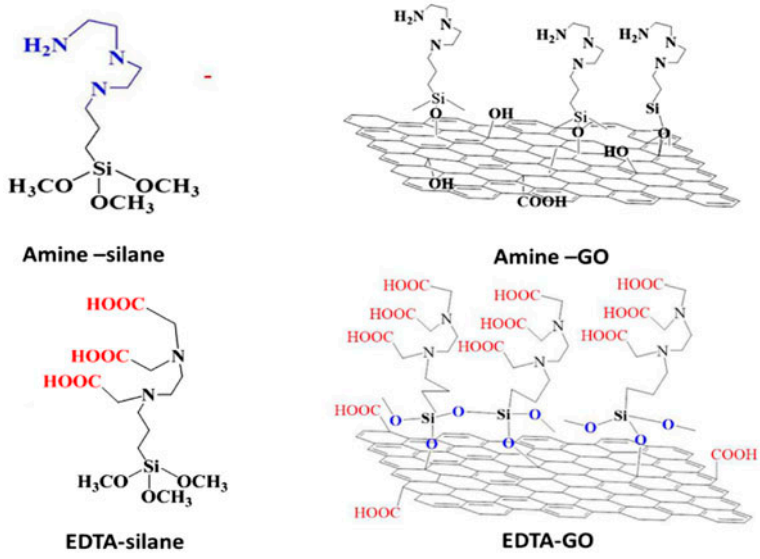

Fig. 1. The chemical structure of amine–silane, EDTA–silane, amine-GO, and EDTA-GO.

was calculated as the difference between initial and remained concentration at a specific time. Finally, the effects of pH on Ni(II) adsorption were measured following the same procedure. Commercial products of AC, GO, and cation-exchange resin were used as control materials to detect the adsorption and desorption behavior after identical conditions.

2.3. Recycle experiments

Recycle experiments were performed utilizing HCl to wash the sorbents after an adsorption process. The amounts of the absorbed Ni(II) (W_{ad}) on EDTA–GO or amine-GO sorbents were calculated from Eq. (2):

$$W_{ad} = (C_i - C_e) \times V \quad (2)$$

where all the parameters were the same as Eq. (1).

After filtering through a 0.2 μm membrane and washing with a buffer solution, the sorbents were dried in an oven at 100°C and then put in a HCl solution of 100 mL with pH values of 2.0, 3.0, 4.0, 5.0, and 6.0, respectively. After treatment for 4 h, Ni(II) adsorbed onto EDTA-GO or amine-GO surface was desorbed and dissolved in HCl solution. The amount of Ni(II) desorbed (released) from the sorbents was used to determine the desorption ratio of Ni(II) onto EDTA-GO or amine-GO sorbent (W_{ds}).

The amount of dissolved Ni(II) into HCl solution was analyzed using ICP. The desorption ratio (α_{ds}) was calculated by the following Eq. (3):

$$\alpha_{ds} = \frac{W_{ds}}{W_{ad}} \quad (3)$$

where W_{ad} was the mass (g) of adsorbed Ni(II) on EDTA-GO and amine-GO sorbents calculated from Eq. (2), and W_{ds} was the mass (g) of the dissolved Ni(II) from EDTA-GO and amine-GO surface into HCl solution. The values of W_{ds} are calculated using the concentration of Ni(II) in the HCl solution.

2.4. Competitive adsorption experiments

The competitive adsorption of various heavy metals onto the EDTA-GO and amine-GO surface was performed by adding 20 mg sample into 20 mL aqueous solution containing 50 ppm of Cu^{2+}, Ni^{2+}, Cd^{2+}, and Fe^{2+}. After filtration and drying in an oven, the filtered EDTA-GO and amine-GO were investigated using SEM and EDXS. The surface element ratio was calculated from the adsorption strength and the data reflected the surface element enrichment.

3. Results and discussion

3.1. FTIR spectra of EDTA-GO, amine-GO, and GO

Fig. 2 shows the FTIR spectra of EDTA-GO, amine-GO, and GO. The absorption band at 1,630 cm^{-1}, observed for all samples, is attributed to the C=C bond of the hexagonal network in GO. The absorption at 1,730 cm^{-1} is attributed to the stretching of the C=O

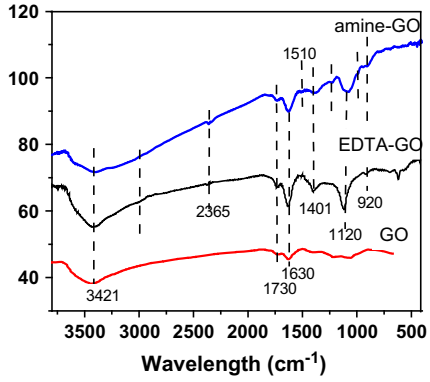

Fig. 2. FTIR spectra of EDTA-GO, amine-GO, and GO.

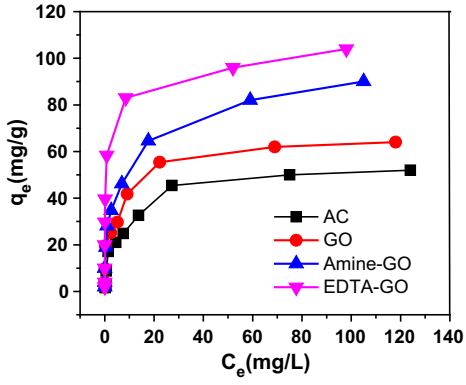

Fig. 3. Adsorptive isotherms of Ni(II) onto AC, GO, EDTA-GO, and amine-GO at pH 6.8 and temperature of (25 ± 2)°C. The initial concentration of Ni(II) was 1–200 mg/L.

bond and the bands around 1,400 cm^{-1} are attributed to the stretching modes of the C–O–H bonds of the carboxylic acid. These contributions confirm the efficiency of the C=O groups which are formed during an oxidizing process of graphite to GO [38,39].

Both EDTA-GO and amine-GO spectra show vibrational modes of the N–H bond at 1,510–1,525 cm^{-1}. This peak is absent for GO. The strength of amine-GO is stronger than that of EDTA-GO. Another important absorption band is the stretching of the C–N bond present in the EDTA-GO and amine-GO molecule at 1,120 cm^{-1} [40,41]. The bands at 920 cm^{-1} for EDTA-GO and amine-GO correspond to the Si–OH vibration, and the bands of EDTA-GO and amine-GO at 1,066 cm^{-1} were assigned to the formation of Si–O–C [42–45]. These characteristics confirm the silanization of GO with amine–silane and EDTA–silane.

3.2. Adsorption capacity

The adsorption isotherms of EDTA-GO, amine-GO, GO, and AC toward Ni(II) from initial solution concentrations ranging from 1 to 200 mg/L are depicted in Fig. 3. The adsorption capacity of Ni(II) onto EDTA-GO is 103 mg/g at an equilibrium concentration of 92 mg/L, while the adsorption capacity for Ni (II) onto amine-GO, GO, and AC is 86 mg/g, 58 mg/g, and 32 mg/g, respectively.

The adsorption capacity of Ni(II) on EDTA-GO and amine-GO is much higher than AC (4.89 mg/g) [46] and other methods (39 and 60.38 mg/g) [47–51]. One of the reasons is because of the higher specific surface area and the functional groups on GO surface. The oxidation process of GO synthesis introduces a high concentration of –OH, –COOH, and C=O groups onto the surface. Another possible binding mechanism of Ni(II) onto EDTA-GO is that the metal ions can react with –COOH and –OH groups on the EDTA-GO surface, either on the graphene sheet or within the EDTA group [52,53]. The complex structure of Ni(II) with EDTA-GO and amine-GO is shown in Fig. 4. The introduced EDTA is an excellent functional group for chelating heavy metal ions.

Langmuir and Freundlich adsorption isotherm models are used to analyze the experimental data for Ni(II) adsorption onto EDTA-GO and amine-GO [54]. Typically, the Langmuir equation can be written as Eq. (4):

$$\frac{1}{q_e} = \frac{1}{q_{\max}} + \frac{1}{q_{\max} \times K_L C_e} \tag{4}$$

where q_e is the adsorption amount of Ni(II) onto the adsorbent (mg/g), $q_{\max}$ is the adsorption capacity of Ni(II) onto the adsorbent (mg/g), C_e is the equilibrium concentration of Ni(II) (mg/g), and K_L is the Langmuir adsorption constant, which is related to the adsorption energy.

Eq. (5) represents the Freundlich model, where q_e and C_e are the same as described above. However, K_f

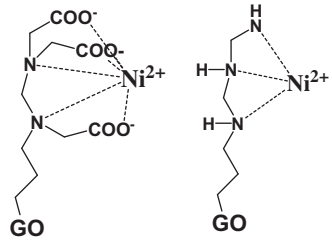

Fig. 4. The complex structure of Ni(II) with EDTA and amine on GO surface.

and n are Freundlich constants relating to adsorption capacity and adsorption intensity, respectively.

$$\log q_e = \log K_F + 1/n \log C_e \quad (5)$$

The detailed experimental data are listed in Table 1. For EDTA-GO, the Langmuir model shows a good agreement with the experimental data, with the correlation coefficient of 0.981 at pH 6.8. And the Freundlich model fits the results well with a correlation coefficient of 0.943, which demonstrates that a monolayer adsorption process at each adsorptive site, such as –COOH, –OH, amine and EDTA groups, can be occupied by heavy metal ions only once in a one-to-one manner.

3.3. The removal efficiency of GO derivatives toward Ni(II) and the influence of pH

One of the important properties to evaluate a sorbent is its removal efficiency. An ideal sorbent should have the capability to release the heavy metal pollutants. Fig. 5 shows the photograph of a series of solutions with indicator and Ni(II) before and after treatment with EDTA-GO, amine-GO, GO, AC, and two commercial resins. It can be seen clearly that Ni (II) can be entirely removed by EDTA-GO and the color of the solution coverts to the initial indicator color. On the contrary, the solution treated with resins is almost the same color as the indicator binding with Ni(II). There is no color observed for the solution treated by AC because AC can adsorb coloured substances [55].

One mechanism to explain this phenomenon is the formation of complex of EDTA with Ni(II), the higher removal efficiency of Ni(II) is probably due to the high formation constant of Ni(II)–EDTA complex [38] (log K = 18.0). The stable complex between EDTA and Ni(II) will contribute to the removal efficiency of EDTA-GO to entirely remove Ni(II) from water system. Table 2 lists the removal efficiency of various lower concentrations of Ni(II) solutions treated with EDTA-GO. It shows that the solution with different concentrations of Ni(II) can reach to a lower level after treating with EDTA-GO. The final concentration of Ni (II) in each solution is 4–65 ppb.

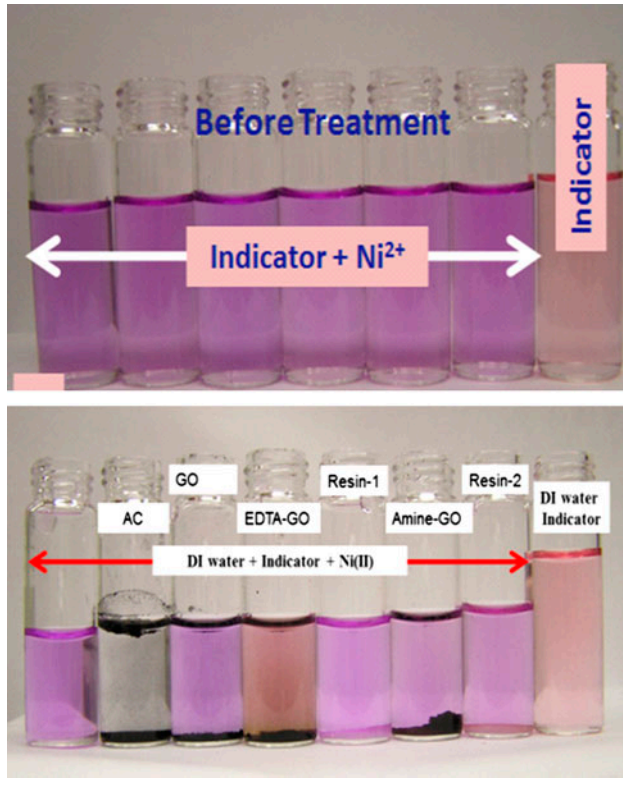

Fig. 5. Photographs of various Ni(II) solutions (A) before and (B) after treatment with various sorbents.

Table 2
The removal efficiency of EDTA-GO towards Ni(II)

Initial concentration of Ni(II) (ppb)					
Initial	10	50	100	500	1,000
Remaining Ni(II) after treated with EDTA-GO (ppb)					
pH 6.2	5.3	12	17.3	55	65
pH 6.8	4.2	8.9	14.0	42	52
pH 7.4	4.2	7.2	10.3	24	44

Condition: 100 mg of EDTA-GO was added to 50.0 mL solutions with different concentrations.

Table 1
Values of the parameters associated with Langmuir and Freundlich models

	Langmuir model			Freundlich model		
	q_e (mg/g)	K_L (L/mg)	R^2	K_F (mg/g(mg/l)^n)	n	R^2
EDTA-GO	103	0.132	0.981	71.66	1.87	0.943
Amine-GO	86	0.028	0.928	10.69	1.24	0.88
GO	58	0.025	0.913	7.38	1.30	0.82

Since there is a complex formation between chelating groups and the metal cations, the pH value of the solution will dramatically affect the adsorption behavior of Ni(II). The pH value effect of EDTA-GO and amine-GO to the adsorption capacities was investigated. Fig. 6 depicts the adsorption capacities of Ni(II) at a concentration of 100 ppm in the pH range of 2.2–9.0. The Ni(II) ions are more favorably absorbed on EDTA-GO and amine-GO at a pH range from 6 to 9.

Two possible mechanisms for the influence of pH on absorption have been suggested. First, the pH values of the solution will affect the surface charge of the GO and the degree of ionization of the heavy metal ions. At a higher pH, the negative charge on the GO surface provides electrostatic interaction, which is favorable for adsorbing cationic species. The decrease of pH leads to neutralization of surface charge and the adsorption efficiency of cations decreases. The increase of the electrostatic forces between $–COO^-$, $–O^-$, and metal cations will result in the increase of uptake capacities for Ni(II). Second, as the pH increases, the formation complex constant between the chelating groups and the heavy metals will increase, and the capacity for heavy metal removal will increase for higher concentration heavy metal solution [52].

For amine-GO, at lower pH value, the removal efficiency of amine-GO is similar to EDTA-GO. The quaternary ammonium groups will be formed and cannot donate electrons, which makes it unable to form complexations with Ni(II) cations. However, some precipitation of $Ni(OH)_2$ will be formed in high pH solution which will interfere with the calculation of the absorption capacity. To avoid the precipitation of metal ions at high pH values, data collection was performed with a pH range of 6.5–7.2. It was believed that, at this pH range, the adsorption uptake reached the maximum due to the effect of the functional groups formed on the GO derivatives surface only.

3.4. Effect of contact time

Compared with 3D sorbents, such as AC and ion exchange resins, the 2D structure of GO enables its functional groups to make direct contact with metal ions, and thus a fast adsorption process is predicted. Fig. 7 demonstrates the adsorption capacities of EDTA-GO reach to the maximum capacity toward Ni (II) with a concentration of 50 mg/L at 35 min and the Ni(II) ions absorbed on amine-GO sorbents reach to the maximum capacities at the same time scale. This rate was faster than most commercial adsorbents [56], which was directly owed to the 2D structure of EDTA-GO and amine-GO. The 2D structure facilitates the adsorbents to be ready for accessibility of the chelating EDTA and amine making them easy for metal chelation.

For the sorption kinetic analysis, 12 h was selected as the sorption time to collect the data for analysis of sorption kinetics, which was enough to reach a sorption equilibrium state. The pseudo-second-order rate Eq. (6) was applied to analyze the kinetic adsorption:

$$\frac{t}{q_t} = \frac{1}{2k'q_e^2} + \frac{t}{q_e} \tag{6}$$

where k' (g/mg/min) was the pseudo-second-order rate constant of adsorption, q_t (mg/g) was the amount of Ni(II) adsorbed on the adsorbent at time t (min), and q_e (mg/g) was the equilibrium

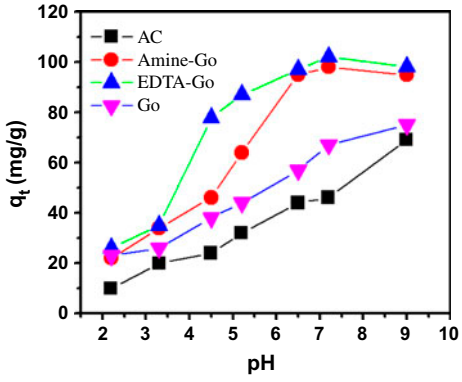

Fig. 6. The effect of pH values on the adsorption capacity of Ni(II) onto four sorbents. The adsorbent dosage was 20 mL/20 mg. Initial concentration of Ni(II) was 100 ppm and temperature was (25 ± 2)°C.

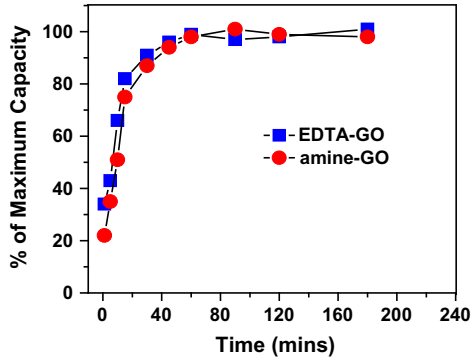

Fig. 7. The effect of contact time on the adsorption capacity of Ni(II) on EDTA-GO and amine-GO. The initial concentration of Ni(II) was 100 ppm, the adsorbent pH was 6.8, and temperature was (25 ± 2)°C.

adsorption capacity. All of the data used here are from Fig. 6. From the linear plot of t/q_t vs t, the k' was estimated to be 0.00084 with a correlation coefficient of 0.9982 (see Table 3) suggesting kinetic adsorption was well described by a pseudo-second-order rate equation.

The adsorption rate with various initial Ni(II) concentrations was investigated. It was found that the adsorption rate was not proportional to the initial heavy metal concentration (C_i). The lower initial concentration resulted in the shorter time to reach the absorption equilibrium state. The possible mechanism was the sorption site adsorbed the available metal ions more rapidly at a lower C_i. For example, the absorption of Ni(II) onto EDTA-GO reached its equilibrium state at ~10, 17, and 22 min at a C_i of 0.03, 0.30, and 1.0 mg/L, respectively. This rate was much faster than other carbon-based adsorbents such as AC, resin, and CNTs [47–51].

3.5. Recycle analysis

Generally, the reusability is one of the most important factors in evaluating an ideal sorbent. A typical recycle process was performed by treating EDTA-GO and amine-GO powder preloaded with Ni(II) with a HCl solution. During the HCl washing process, Ni(II) on EDTA-GO and amine-GO surface was released into solution. Fig. 8 illustrates the desorption ratio of Ni(II) absorbed onto EDTA-GO and amine-GO surface as a function of pH. It was apparent that desorption ratio of Ni(II) increased with the decrease in pH values of HCl solution. When the pH value of the HCl solution was greater than 5, only 15% of the adsorbed Ni(II) was desorbed from the EDTA-GO surface. The desorption ratio increased with high concentration of HCl, and reached to 50% and above when the pH value of the HCl solution was lower than 3.0. The desorption ratio eventually reached to about 90% when the pH value of the HCl solution was 1.0 (0.10 M HCl). We note that amine-GO presented the same trend.

Fig. 9 demonstrates the reusability of EDTA-GO and amine-GO toward the removal of Ni(II). It was shown that both EDTA-GO and amine-GO exhibit good performance characteristics after 20 wash recycles. After 20 cycles, 80% of the initial adsorption capacity of EDTA-GO remained and 87% of the initial adsorption capacity of amine-GO remained.

Table 3
Values of the parameters associated with pseudo-second-order adsorption

	C	q_e	k'	R
EDTA-GO	50 ppm	105	0.00084	0.9982
Amine-GO		93	0.00069	0.9723

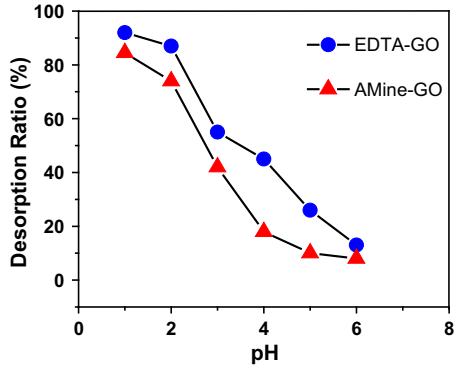

Fig. 8. The desorption ratio of EDTA-GO and amine-GO with Ni(II). The adsorbent dosage was 100 mg/100 mL and initial concentration of Ni was 200 mg/mL.

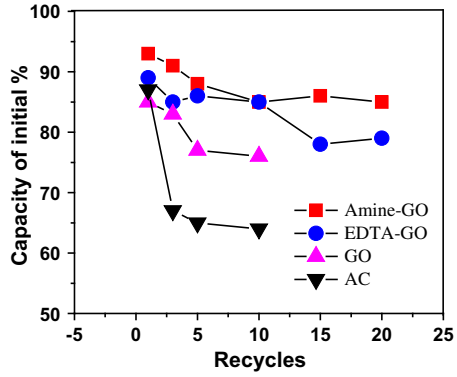

Fig. 9. The adsorption capacities of Ni(II) after HCl washing for different adsorbents.

3.6. The adsorption selectivity

In a real wastewater system, Ni(II) always coexists with other metal ions, including Cu^{2+}, Cd^{2+}, and Fe^{2+}. The effects of competitive ions on the adsorption of Ni (II) was simulated and the selectivity of the EDTA-GO and amine-GO toward the adsorption of Cu^{2+}, Ni^{2+}, Cd^{2+}, and Fe^{2+} was investigated. Fig. 10 demonstrates the EDXS element analysis results of EDTA-GO and amine-GO samples treated with a solution containing 50 ppm of Cu^{2+}, Ni^{2+}, Cd^{2+}, and Fe^{2+}, respectively. The percentages of the metal elements on GO surface are depicted. It was determined that when the four

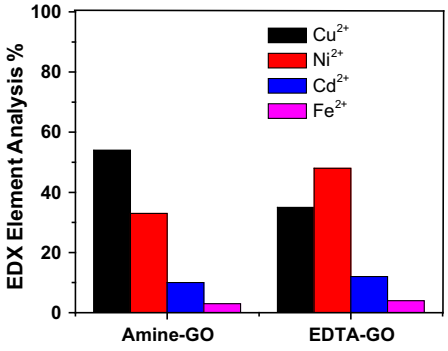

Fig. 10. The EDX element analysis of heavy metals on EDTA-GO and amine-GO surface. Initial concentrations of Cu^{2+}, Ni^{2+}, Cd^{2+}, and Fe^{2+} were 50 ppm and temperature was (25 ± 2)°C.

metal ions co-existed at the same concentration, the percentage of Ni(II) on EDTA-GO surface (48%) was higher than all of the other three ions, which proved that EDTA-GO was a good sorbent for Ni(II) removal in a mixture solution. On the contrary, the percentage of Cu(II) on amine-GO surface (52%) was higher than all other three ions predicting that amine-GO could be a good sorbent for Cu(II) removal in mixture solution.

4. Conclusions

The chelating groups, such as EDTA and amine, linked to the GO surface, can significantly increase the adsorption capacity and the removal efficiency toward the heavy metal pollutants. The maximum adsorption capacities of EDTA-GO and amine-GO for Ni(II) are 103 and 86 mg/g, respectively, which are higher than that of GO, AC, and other commercial products. The adsorption behavior of Ni(II) on EDTA-GO fits the Langmuir equation well. The adsorption capacity varies with the pH value of the solution and these sorbents can be reused after washing with 0.10 M HCl. This research demonstrates that EDTA-GO and amine-GO can be designed as very effective sorbents for heavy metal removal.

Acknowledgments

The authors are grateful for the financial support of the National Natural Science Foundation of China (21375076, 21275089, and 21403124), the Scientific Research Starting Foundation for Returned Overseas (Ministry of Education of China), and the Project of Shandong Province Science and Technology Program (2013GGX10207).

References

[1] A.A. Juwarkar, S.K. Singh, A comprehensive overview of elements in bioremediation, Rev. Environ. Sci. Bio/Technol. 9 (2010) 215–288.
[2] P.K. Tapaswi, M.S. Moorthy, S.S. Park, Fast, selective adsorption of Cu^{2+} from aqueous mixed metal ions solution using 1,4,7-triazacyclononane modified SBA-15 silica adsorbent (SBA-TACN), J. Solid State Chem. 211 (2014) 191–199.
[3] F.A. Abu Al-Rub, M. Kandah, N. Al-Dabaybeh, Competitive adsorption of nickel and cadmium on sheep manure wastes: Experimental and prediction studies, Sep. Sci. Technol. 38 (2003) 483–497.
[4] D.L. Guerra, V.L. Leidens, R.R. Viana, C. Airoldi, Application of Brazilian kaolinite clay as adsorbent to removal of U(VI) from aqueous solution: Kinetic and thermodynamic of cation–basic interactions, J. Solid State Chem. 183 (2010) 1141–1149.
[5] F.L. Fu, Q. Wang, Removal of heavy metal ions from wastewaters: A review, J. Environ. Manage. 92 (2011) 407–418.
[6] S.H. Lin, S.L. Lai, H.G. Leu, Removal of heavy metals from aqueous solution by chelating resin in a multi-stage adsorption process, J. Hazard. Mater. 76 (2000) 139–153.
[7] G. Zhao, X. Wu, X. Tan, X. Wang, Sorption of heavy metal ions from aqueous solutions: A review, Open Colloid Sci. J. 4 (2011) 19–31.
[8] M.S. Mauter, M. Elimelech, Environmental applications of carbon-based nanomaterials, Environ. Sci. Technol. 42 (2008) 5843–5859.
[9] L.E. Macaskie, I.P. Mikheenko, P. Yong, K. Deplanche, A.J. Murray, M. Paterson-Beedle, V.S. Coker, C.I. Pearce, R. Cutting, R.A.D. Pattrick, D. Vaughan, G. van der Laan, J.R. Lloyd, Today's wastes, tomorrow's materials for environmental protection, Hydrometallurgy 104 (2010) 483–487.
[10] T. Pradeep, Anshup, Noble metal nanoparticles for water purification: A critical review, Thin Solid Films 517 (2009) 6441–6478.
[11] J.P. Ruparelia, S.P. Duttagupta, A.K. Chatterjee, S. Mukherji, Potential of carbon nanomaterials for removal of heavy metals from water, Desalination 232 (2008) 145–156.
[12] J.Hu, D.D. Shao, C.L. Chen, G.D. Sheng, J.X. Li, X.K. Wang, M. Nagatsu, Plasma-induced grafting of cyclodextrin onto multiwall carbon nanotube/iron oxides for adsorbent application, J. Phys. Chem. B 114 (2010) 6779–6785.
[13] H. Wang, L. Wang, C.Q. Qu, Y.D. Su, S.S. Yu, W.T. Zheng, Y.C. Liu, Photovoltaic properties of graphene oxide sheets beaded with ZnO nanoparticles, J. Solid State Chem. 184 (2011) 881–887.
[14] Y.J. Liu, M. Aizawa, W.Q. Peng, Z.M. Wang, T. Hirotsu, Carbon nanosheet-titania nanocrystal composites from reassembling of exfoliated graphene oxide layers with colloidal titania nanoparticles, J. Solid State Chem. 197 (2013) 329–336.
[15] D.R. Dreyer, S. Park, C.W. Bielawski, R.S. Ruoff, The chemistry of graphene oxide, Chem. Soc. Rev. 39 (2010) 228–240.
[16] J. Li, S.W. Zhang, C.L. Chen, G.X. Zhao, X. Yang, J.X. Li, X.K. Wang, Removal of Cu(II) and fulvic acid by

graphene oxide nanosheets decorated with Fe_3O_4 nanoparticles, ACS Appl. Mater. Interfaces 4 (2012) 4991–5000.
[17] X. Yang, C.L. Chen, J.X. Li, G.X. Zhao, X.M. Ren, X.K. Wang, Graphene oxide-iron oxide and reduced graphene oxide-iron oxide hybrid materials for the removal of organic and inorganic pollutants, RSC Adv. 2 (2012) 8821–8826.
[18] M.C. Liu, C.L. Chen, J. Hu, X.L. Wu, X.K. Wang, Synthesis of magnetite/graphene oxide composite and application for cobalt(II) removal, J. Phys. Chem. C 115 (2011) 25234–25240.
[19] G.X. Zhao, X.M. Ren, X. Gao, X.L. Tan, J.X. Li, C.L. Chen, Y.Y. Huang, X.K. Wang, Removal of Pb(II) ions from aqueous solutions on few-layered graphene oxide nanosheets, Dalton Trans. 40 (2011) 10945–10952.
[20] C.W. Bielawski, D.R. Dreyer, R.S. Ruoff, From conception to realization: An historial account of graphene and some perspectives for its future, Angew. Chem. Int. Ed. 49 (2010) 9336–9344.
[21] T.S. Sreeprasad, S.M. Maliyekkal, K.P. Lisha, T. Pradeep, Reduced graphene oxide–metal/metal oxide composites: Facile synthesis and application in water purification, J. Hazard. Mater. 186 (2011) 921–931.
[22] X.J. Deng, L.L. Lü, H.W. Li, F. Luo, The adsorption properties of Pb(II) and Cd(II) on functionalized graphene prepared by electrolysis method, J. Hazard. Mater. 183 (2010) 923–930.
[23] S.T. Yang, Y.L. Chang, H.F. Wang, G.B. Liu, S. Chen, Y.W. Wang, Y.F. Liu, A.N. Cao, Folding/aggregation of graphene oxide and its application in Cu^{2+} removal, J. Colloid Interface Sci. 351 (2010) 122–127.
[24] C. Petit, B. Mendoza, T.J. Bandosz, Hydrogen sulfide adsorption on MOFs and MOF/graphite oxide composites, ChemPhysChem 11 (2010) 3678–3684.
[25] C. Petit, B. Mendoza, T.J. Bandosz, Reactive adsorption of ammonia on Cu-based MOF/graphene composites, Langmuir 26 (2010) 15302–15309.
[26] T. Zhang, Z.G. Cheng, Y.B. Wang, Z.J. Li, C.X. Wang, Y.B. Li, Y. Fang, Self-assembled 1-octadecanethiol monolayers on graphene for mercury detection, Nano Lett. 10 (2010) 4738–4741.
[27] W. Gao, M. Majumder, L.B. Alemany, T.N. Narayanan, M.A. Ibarra, B.K. Pradhan, P.M. Ajayan, Engineered graphite oxide materials for application in water purification, ACS Appl. Mater. Interfaces 3 (2011) 1821–1826.
[28] G. Gollavelli, C.C. Chang, Y.C. Ling, Facile synthesis of smart magnetic graphene for safe drinking water: Heavy metal removal and disinfection control, ACS Sustainable Chem. Eng. 1 (2013) 462–472.
[29] H. Gao, Y. Sun, J. Zhou, R. Xu, H. Duan, Mussel-inspired synthesis of polydopamine-functionalized graphene hydrogel as reusable adsorbents for water purification, ACS Appl. Mater. Interfaces 5 (2013) 425–432.
[30] C.Y. Cao, J. Qu, F. Wei, H. Liu, W.G. Song, Superb adsorption capacity and mechanism of flowerlike magnesium oxide nanostructures for lead and cadmium ions, ACS Appl. Mater. Interfaces 4 (2012) 4283–4287.
[31] V. Chandra, J. Park, Y. Chun, J.W. Lee, I.C. Hwang, K.S. Kim, Water-dispersible magnetite-reduced graphene oxide composites for arsenic removal, ACS Nano 4 (2010) 3979–3986.
[32] Y. Ren, N. Yan, Q.Z. Wen, Zhuangjun Fan, Tong Wei, Milin Zhang, Graphene/δ-MnO_2 composite as adsorbent for the removal of nickel ions from wastewater, Chem. Eng. J. 175 (2011) 1–7.
[33] S.F. Hou, S.J. Su, M.L. Kasner, P. Shah, K. Patel, C.J. Madarang, Formation of highly stable dispersions of silane-functionalized reduced graphene oxide, Chem. Phys. Lett. 501 (2010) 68–74.
[34] S.F. Hou, M.L. Kasner, S.J. Su, K. Patel, R. Cuellari, Highly sensitive and selective dopamine biosensor fabricated with silanized graphene, J. Phys. Chem. C 114 (2010) 14915–14921.
[35] M.S. Wietecha, J. Zhu, G. Gao, N. Wang, H. Feng, M.L. Gorring, M.L. Kasner, S. Hou, Platinum nanoparticles anchored on chelating group-modified graphene for methanol oxidation, J. Power Sources 198 (2012) 30–35.
[36] C.J. Madadrang, H.Y. Kim, G. Gao, N. Wang, J. Zhu, H. Feng, M. Gorring, M.L. Kasner, S. Hou, Adsorption behavior of EDTA-graphene oxide for Pb(II) removal, ACS Appl. Mater. Interfaces 4 (2012) 1186–1193.
[37] W.S. Hummers, R.E. Offeman, Preparation of graphitic oxide, J. Am. Chem. Soc. 80 (1958) 1339.
[38] K.J. Huang, D.J. Niu, X. Liu, Z.W. Wu, Y. Fan, Y.F. Chang, Y.Y. Wu, Direct electrochemistry of catalase at amine-functionalized graphene/gold nanoparticles composite film for hydrogen peroxide sensor, Electrochimica Acta 56 (2011) 2947–2953.
[39] W.M. Silva, H. Ribeiro, L.M. Seara, H.D.R. Calado, A.S. Ferlauto, R.M. Paniago, C.F. Leite, G.G. Silva, Surface properties of oxidized and aminated multiwalled carbon nanotubes, J. Braz. Chem. Soc. 23 (2012) 1078–1086.
[40] S. Yuen, C.C.M. Ma, C.L. Chiang, Silane grafted MWCNT/polyimide composites preparation, morphological and electrical properties, Compos. Sci. Technol. 68 (2008) 2842–2848.
[41] H. Yang, F. Li, C. Shan, D. Han, Q. Zhang, L. Niu, A. Ivaska, Covalent functionalization of chemically converted graphene sheets via silane and its reinforcement, J. Mater. Chem. 19 (2009) 4632–4638.
[42] P.C. Ma, J.K. Kim, B.Z. Tang, Functionalization of carbon nanotubes using a silane coupling agent, Carbon 44 (2006) 3232–3238.
[43] P.C. Ma, J.K. Kim, B.Z. Tang, Effects of silane functionalization on the properties of carbon nanotube/epoxy nanocomposites, Compos. Sci. Technol. 67 (2007) 2965–2972.
[44] T. Hemraj-Benny, S.S. Wong, Silylation of single-walled carbon nanotubes, Chem. Mater. 18 (2006) 4827–4839.
[45] Masami Aizawa, Milo S.P. Shaffer, M.S.P. Shaffer, Silylation of multi-walled carbon nanotubes, Chem. Phys. Lett. 368 (2003) 121–124.
[46] H. Hasar, Adsorption of nickel (II) from aqueous solution onto activated carbon prepared from almond husk, J. Hazard. Mater. 97 (2003) 49–57.
[47] K. Vijayaraghavan, J. Jegan, K. Palanivelu, M. Velan, Biosorption of cobalt(II) and nickel(II) by seaweeds: Batch and column studies, Sep. Purif. Technol. 44 (2005) 53–59.
[48] K. Vijayaraghavan, J. Jegan, K. Palanivelu, M. Velan, Removal of nickel (II) ions from aqueous solution using crab shell particles in a packed bed up-flow column, J. Hazard. Mater. 113 (2004) 223–230.

[49] Z. Aksu, D. Akpınar, Modelling of simultaneous biosorption of phenol and nickel (II) onto dried aerobic activated sludge, Sep. Purif. Technol. 21 (2000) 87–99.
[50] N. Akhtar, J. Iqbal, M. Iqbal, Removal and recovery of nickel (II) from aqueous solution by loofa sponge-immobilized biomass of Chlorella sorokiniana: Characterization studies, J. Hazard. Mater. 108 (2004) 85–94.
[51] S. Al-Asheh, F. Banat, F. Mohai, Sorption of copper and nickel by spent animal bones, Chemosphere 39 (1999) 2087–2096.
[52] E. Repo, T.A. Kurniawan, J.K. Warchol, M.E.T. Sillanpää, Removal of Co(II) and Ni(II) ions from contaminated water using silica gel functionalized with EDTA and/or DTPA as chelating agents, J. Hazard. Mater. 171 (2009) 1071–1080.
[53] K. Kadirvelu, C. Faur-Brasquet, P. Cloirec, Removal of Cu(II), Pb(II), and Ni(II) by adsorption onto activated carbon cloths, Langmuir 16 (2000) 8404–8409.
[54] G.D. Vuković, A.D. Marinković, M. Čolić, M.D. Ristić, R. Aleksić, A.A. Perić-Grujić, P.S. Uskoković, Removal of cadmium from aqueous solutions by oxidized and ethylenediamine-functionalized multi-walled carbon nanotubes, Chem. Eng. J. 157 (2010) 238–248.
[55] H. Métivier-Pignon, C. Faur-Brasquet, P. Le Cloirec, Adsorption of dyes onto activated carbon cloths: Approach of adsorption mechanisms and coupling of ACC with ultrafiltration to treat coloured wastewaters, Sep. Purif. Technol. 31 (2003) 3–11.
[56] M.F. Taha, C.F. Kiat, M.S. Shaharun, A. Ramli. Removal of Ni(II), Zn(II) and Pb(II) ions from single metal aqueous solution using activated carbon prepared from rice husk, World Acad. Sci., Eng. Technol. 60 (2011) 291–296.